Beam-Recoil Polarization Measurement of π^0 Electroproduction on the Proton in the Region of the Roper Resonance

S. Štajner,[1] P. Achenbach,[2] T. Beranek,[2] J. Beričič,[1] J. C. Bernauer,[3] D. Bosnar,[4] R. Böhm,[2] L. Correa,[5] A. Denig,[2] M. O. Distler,[2] A. Esser,[2] H. Fonvieille,[5] J. M. Friedrich,[6] I. Friščić,[4,†] S. Kegel,[2] Y. Kohl,[2] H. Merkel,[2] M. Mihovilovič,[1,2] J. Müller,[2] U. Müller,[2] L. Nungesser,[2] J. Pochodzalla,[2] B. S. Schlimme,[2] M. Schoth,[2] F. Schulz,[2] C. Sfienti,[2] S. Širca,[7,1,*] M. Thiel,[2] L. Tiator,[2] A. Tyukin,[2] A. Weber,[2] and I. Yaron[8]

(A1 Collaboration)

[1]*Jožef Stefan Institute, SI-1000 Ljubljana, Slovenia*
[2]*Institut für Kernphysik, Johannes Gutenberg-Universität Mainz, DE-55128 Mainz, Germany*
[3]*Massachusetts Institute of Technology, Cambridge, Massachusetts 02139, USA*
[4]*Department of Physics, Faculty of Science, University of Zagreb, HR-10002 Zagreb, Croatia*
[5]*Université Clermont Auvergne, CNRS/IN2P3, LPC, F-63000 Clermont-Ferrand, France*
[6]*Technische Universität München, Physik Department, 85748 Garching, Germany*
[7]*Faculty of Mathematics and Physics, University of Ljubljana, SI-1000 Ljubljana, Slovenia*
[8]*School of Physics and Astronomy, Tel Aviv University, Tel Aviv 69978, Israel*

(Received 15 March 2017; revised manuscript received 22 May 2017; published 13 July 2017)

The helicity-dependent recoil proton polarizations P'_x and P'_z as well as the helicity-independent component P_y have been measured in the $p(\vec{e}, e'\vec{p})\pi^0$ reaction at four-momentum transfer $Q^2 \simeq 0.1$ GeV^2, center-of-mass proton emission angle $\theta^*_p \simeq 90°$, and invariant mass $W \simeq 1440$ MeV. This first precise measurement of double-polarization observables in the energy domain of the Roper resonance $P_{11}(1440)$ by exploiting recoil polarimetry has allowed for the extraction of its scalar electroexcitation amplitude at an unprecedentedly low value of Q^2, establishing a powerful instrument for probing the interplay of quark and meson degrees of freedom in the nucleon.

DOI: 10.1103/PhysRevLett.119.022001

Electromagnetic production of pseudoscalar mesons on free protons is a most sensitive and efficient tool to explore the structure of nucleon resonances [1,2]. Among them, the nature of the Roper resonance has been the subject of a heated debate ever since its discovery in the isospin-1/2, spin-1/2 partial wave of πN scattering [3]. Although it is the first excitation of the proton with the same quantum numbers, it remains poorly understood in comparison with the thoroughly studied $\Delta(1232)$ resonance in the isospin-3/2, spin-3/2 channel.

Buried deep under the tails of neighboring excitations, the Roper resonance has been unambiguously observed in πN scattering, yet modern partial-wave analyses [4–6] still yield strongly disparate positions and widths with a nontrivial structure of the poles in the complex energy plane, indicating that its Breit-Wigner interpretation is far from adequate. The search for the Roper resonance is also one of the prominent challenges of lattice QCD: Although the picture seems to be clearing slowly [7], new caveats keep on emerging [8].

Identifying the manifestations of the Roper resonance in processes induced by real or virtual photons has proven to be difficult, in part due to the relative complexity of its decay channels and their uncertain branching fractions. There is a large body of data on pion and two-pion electroproduction processes in the energy region of the Roper resonance; see, for example, Refs. [9–14]. In some cases, single-spin and beam-target double-spin asymmetries have been measured but with the significant drawback that the target could always be polarized only along the direction of the incoming electron. A relevant advantage of our experiment is the liberty to produce and measure precisely any recoil polarization. Admittedly, the experiment in which the beam and the target are polarized gives access to the same physics content as those involving polarized beams and recoil polarization determination, but, although the techniques are believed to be theoretically equivalent [15], these two approaches have never been cross-checked in the energy region of the Roper resonance and are subject to entirely different systematics. Because of this complementarity and their extreme sensitivity and capability to stabilize phenomenological fits, Roper-related recoil polarization observables also represent crucial testing grounds for the state-of-the-art models like MAID [16], DMT [17], and SAID [18], representing distinct approaches to meson electroproduction calculations ranging from unitary isobar models operating with dressed resonances versus dynamical models incorporating bare states and their subsequent dynamical dressing to full-scale partial-wave analysis of scattering and photo- or electroproduction processes.

Only a handful of experiments on pseudoscalar meson production involving recoil proton polarization analysis have been performed so far: The $p(\vec{e},e'\vec{p})\pi^0$ process in the region of the $\Delta(1232)$ resonance has been studied at the Mainz Microtron (MAMI) facility in Mainz [19] and at Jefferson Lab [20,21]. The $p(\vec{e},e'\vec{p})\eta$ process in the vicinity of the $S_{11}(1535)$ resonance has also been investigated at MAMI [22]. No such measurement has ever been performed in the region of the Roper resonance, in particular, at low-momentum transfers where the effects of the pion cloud are expected to be most relevant. The aim of this experiment was to provide precise beam-recoil double-polarization data for the $p(\vec{e},e'\vec{p})\pi^0$ process in this particular regime.

The differential cross section for the $p(\vec{e},e'\vec{p})\pi^0$ process involving beam polarization and recoil polarization analysis can be cast in the form [23]

$$\frac{d^5\sigma}{dp'_e d\Omega'_e d\Omega^*_p} = \Gamma\bar{\sigma}(1 + hA + \boldsymbol{S}\cdot\boldsymbol{\Pi}),$$

where Γ is the virtual photon flux, $\bar{\sigma}$ is the unpolarized cross section, h is the electron helicity, A is the beam-analyzing power (equal to zero assuming parity invariance), $\boldsymbol{S}$ is the spin direction for the recoil proton, and $\Pi = \boldsymbol{P} + h\boldsymbol{P}'$ is the recoil polarization consisting of its helicity-independent and helicity-dependent parts. The polarization vectors are expressed in the basis defined by the unit vectors $\hat{\ell}$, $\hat{n}$, and $\hat{t}$, where $\hat{\ell}$ is along the final nucleon momentum in the center-of-mass (c.m.) frame, $\hat{n} \propto \hat{q}\times\hat{\ell}$ is normal to the reaction plane, and $\hat{t} = \hat{n}\times\hat{\ell}$.

The cross section can be decomposed into products of exactly calculable kinematic factors ν_α, depending only on electron kinematics (see Ref. [20] for their functional forms), with the response functions R_α, which carry the relevant hadronic information. The central kinematics of the present experiment has been chosen such that $\theta^*_p \approx 90°$ and $\phi^*_p \approx 0°$ (in-plane measurement), resulting in three nonvanishing polarization components:

$$P'_\ell\bar{\sigma} = \nu_0[\nu_{LT'}R^\ell_{LT'} + \nu_{TT'}R^\ell_{TT'}],$$
$$P_n\bar{\sigma} = \nu_0[\nu_L R^n_L + \nu_T R^n_T + \nu_{LT}R^n_{LT} + \nu_{TT}R^n_{TT}],$$
$$P'_t\bar{\sigma} = \nu_0[\nu_{LT'}R^t_{LT'} + \nu_{TT'}R^t_{TT'}],$$

where $\bar{\sigma} = \nu_0[\nu_L R_L + \nu_T R_T + \nu_{LT}R_{LT} + \nu_{TT}R_{TT}]$. In the specific kinematics of our experiment, these polarization components are related to the components in the frame of the scattering plane by $P'_x = -P'_l$, $P_y = P_n$, and $P'_z = -P'_t$, which will be used to present the results.

The structure functions can be further represented in terms of the bilinear forms of electroproduction multipoles. For the Roper resonance, the multipoles of interest are the scalar (monopole) S_{1-} and the magnetic dipole M_{1-}. To leading orders in the angular decomposition, the relevant terms in the structure functions are

$$R^\ell_{TT'} \propto \mathrm{Re}E^*_{0+}(3E_{1+} + M_{1+} + 2M_{1-}),$$
$$R^n_T \propto \mathrm{Im}E^*_{0+}(3E_{1+} + M_{1+} + 2M_{1-});$$

hence, P'_l and P_n pick up the real and imaginary parts, respectively, of the same interference of the nonresonant E_{0+} multipole with the resonant M_{1-}. These interferences are the key to the sensitivity of our experiment to its Roper content as a small resonant amplitude is multiplied by a large nonresonant one. By the same token, since $R^\ell_{LT'} \propto \mathrm{Re}S^*_{1-}M_{1-}$ and $R^n_{LT} \propto \mathrm{Im}S^*_{1-}M_{1-}$, the same polarization components are also sensitive to the respective resonant-resonant interferences, but these terms are correspondingly smaller. As $P'_t \propto R^t_{LT'}$, the transverse component P'_t is sensitive to two interference terms involving resonant and nonresonant amplitudes:

$$R^t_{LT'} \propto \mathrm{Re}[S^*_{0+}(2M_{1+} + M_{1-}) + (2S^*_{1+} - S^*_{1-})E_{0+}].$$

Our experimental study of the $p(\vec{e},e'\vec{p})\pi^0$ process was performed at the three-spectrometer facility of the A1 Collaboration [24] at MAMI [25,26]. The kinematic ranges covered by our experiment were $W \approx (1440 \pm 40)$ MeV for the invariant mass, $\theta^*_p \approx (90 \pm 15)°$ and $\phi^*_p \approx (0 \pm 30)°$ for the c.m. scattering angles, and $Q^2 \approx (0.1 \pm 0.02)$ $(\mathrm{GeV}/c)^2$ for the square of the four-momentum transfer.

The incident electron beam had an energy of 1508 MeV and had an average degree of polarization of 87% and a charge asymmetry of about 10^{-4}. An average beam current of 15 μA was delivered on a liquid hydrogen target with a length of 5 cm. In order to avoid local boiling effects, the beam was rastered across the target. Spectrometer A was employed as the recoil proton arm, since it has the capability to analyze the recoil polarization with its dedicated focal-plane polarimeter system (FPP) [27]. The electrons were detected with spectrometer B in coincidence with the proton arm. All spectrometers are equipped with four layers of vertical drift chambers (VDCs) and two layers of plastic scintillation detectors. Spectrometer B also contained a Cherenkov detector to positively identify electrons, while spectrometer A had the FPP in its place to allow for proton polarimetry. The VDCs were used for particle tracking, while scintillation detectors provided timing information and particle identification. The FPP consisted of the 7-cm-thick carbon scatterer and the horizontal drift chamber package providing the information on secondary scattering needed for the measurement of the proton spin near the focal plane of the spectrometer.

Because of the good time-of-flight resolution (0.9 ns FWHM) for the coincidence time peak, no further particle identification conditions were necessary. Background events were further reduced by cutting on the clear neutral pion peak in the missing mass spectrum. This, along with the cuts on track reconstruction quality, allowed for the selection of clean FPP events. Only events with secondary

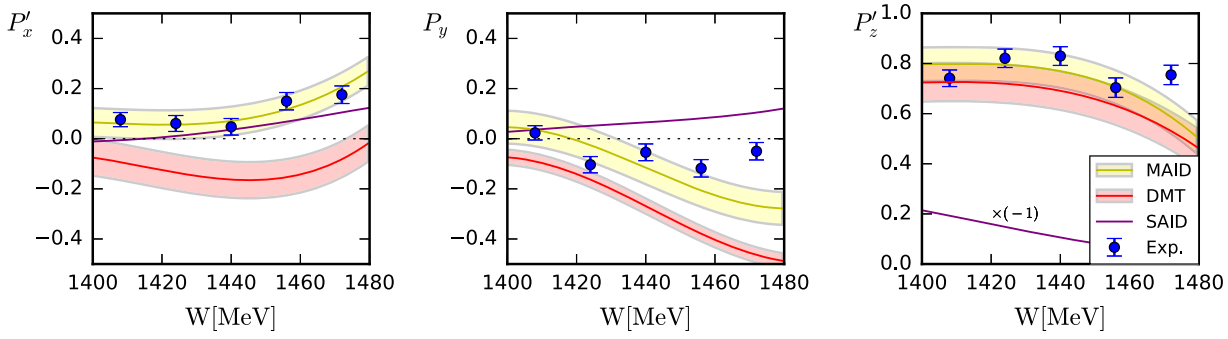

FIG. 1. Recoil proton polarization components as a function of the invariant mass in the vicinity of the Roper resonance, compared to MAID [16] and DMT [17] models and the partial-wave analysis of SAID [18]. Only statistical uncertainties are shown. For systematical uncertainties, see Table I. The shaded bands indicate one-σ uncertainties on the calculations due to acceptance averaging.

scattering angles above 7° where the proton-carbon analysis reaction occurs were selected, yielding a total sample of nearly 100 000 events for polarization analysis.

After detector calibration and event selection, the polarization components measured by the FPP need to be mapped to the components at the primary vertex. This has been accomplished by performing a maximum-likelihood analysis of the transport of estimated target c.m. polarizations to the focal plane and adjusting them in order to find the maximum of the likelihood function [22,28,29]. Since the FPP delivers only two independent components, while we require three components at the target, the likelihood method provides a more reliable approach for the extraction of P'_x, P_y, and P'_z than the traditional reconstruction of the target values from the azimuthal (ϕ_p^{fp}) asymmetries in the FPP [19,27].

The focal plane polarization $\boldsymbol{P}^{\mathrm{fp}}$ can be calculated on an event-by-event basis by a Wigner rotation of the target c.m. polarization into the laboratory frame and by tracing the proton's spin precession from the target to the focal plane through the magnetic field of the spectrometer. The ϕ_p^{fp} dependence of secondary scattering (proton kinetic energies of about 180 MeV) is a known function of $\boldsymbol{P}^{\mathrm{fp}}$ and the local carbon analyzing power [27]. This distribution can be expressed as a probability density function corresponding to the c.m. polarization components at the target, $f(\phi^{\mathrm{fp}}; P'_x, P_y, P'_z)$ [29], which was used to maximize the log-likelihood function $\log L = \sum_i \log f(\phi_{p,i}^{\mathrm{fp}}; P'_x, P_y, P'_z)$. The statistical errors have been determined from the diagonal elements of the covariance matrix of the maximum-likelihood fit. Its off-diagonal elements were at least an order of magnitude smaller than the diagonal terms, implying negligible correlations. This resulted in the best estimate for the acceptance-averaged c.m. polarizations of the recoil protons, shown in Fig. 1.

The error bars on the data in Fig. 1 show only the statistical uncertainties obtained from the maximum-likelihood fit. The transport of the particle's spin from the target to the focal plane contributes to a systematic uncertainty not encapsulated in the error arising from the fit procedure. This error is greatest for P'_z but can be observed in the remaining two components as well. This error originates in the rotation matrix responsible for transforming $\boldsymbol{\Pi}^{\mathrm{cm}}$ into $\boldsymbol{P}^{\mathrm{fp}}$. Since only two independent components can be determined at the focal plane, the likelihood function relies on the nondiagonal elements for the reconstruction of P'_z. These were found to be correlated to P_y in an acceptance-asymmetrical manner, inducing a systematic error [28]. In addition, systematic uncertainties due to the carbon analyzing power are present, as well as the uncertainty on the beam polarization which appears in P'_x and P'_z but not in P_y. Table I summarizes the final experimental results and their uncertainties.

In order to compare our results to two state-of-the-art models in this energy region, MAID [16] and DMT [17], a Monte Carlo simulation with the target polarization input from both models has been made. We have simulated the full reaction process, followed by the particle transport and detection. When the outgoing proton is generated, it is assigned a spin as predicted by the model under consideration and transported to the FPP where a secondary scattering event is simulated. The sample thus generated is structurally equivalent to the experimental one and is further analyzed by using the same methods as the true

TABLE I. The polarization components extracted in five bins of the total energy range of the experiment.

W[MeV]	1408	1424	1440	1456	1472
P'_x	0.08	0.06	0.05	0.15	0.18
$\Delta P'_x$ (stat)	0.03	0.03	0.03	0.04	0.04
$\Delta P'_x$ (syst)	0.01	0.01	0.01	0.02	0.02
P_y	0.02	−0.10	−0.05	−0.12	−0.05
ΔP_y (stat)	0.03	0.03	0.03	0.03	0.03
ΔP_y (syst)	0.02	0.03	0.03	0.02	0.02
P'_z	0.74	0.82	0.83	0.70	0.75
$\Delta P'_z$ (stat)	0.03	0.04	0.04	0.04	0.04
$\Delta P'_z$ (syst)	0.07	0.08	0.08	0.07	0.08

experimental data. The final acceptance-averaged recoil polarizations at the interaction point as predicted by the models are represented as confidence bands in Fig. 1. With the possible exception of P_y at high W, which is reproduced by neither of the models, MAID is in very good agreement with the data, while DMT underestimates all three polarization components and even misses the sign of P'_x. The SAID analysis agrees less well with the P'_x data, while it exhibits an opposite trend in P_y and is completely at odds regarding P'_z. This might be a consequence of very different databases used in the analysis and calls for further investigations within these groups.

Our measurements have also opened a specific path to access the scalar helicity amplitude $S_{1/2}$. This amplitude, in addition to its transverse counterpart $A_{1/2}$, describes the resonance excitation itself, i.e., only the electromagnetic vertex γpN^*. While $A_{1/2}(Q^2 = 0)$ can be determined (and is relatively well known) from photoproduction measurements [30], the $S_{1/2}$ is accessible exclusively in electroproduction ($Q^2 \neq 0$) and becomes increasingly difficult to extract at small Q^2. This is a highly relevant kinematic region where many proposed explanations of the structure of the Roper resonance and mechanisms of its excitation give completely different predictions. For example, the Roper could be a hybrid (q^3g) state, implying a vanishing $S_{1/2}(Q^2)$ [31–35], or a radial excitation (a "breathing mode") of the three-quark core as supported by the observed behavior of $A_{1/2}(Q^2)$ [9,11,36]. This is also a region in which large pion-cloud effects are anticipated [37,38]. The range of theoretical predictions for $S_{1/2}(Q^2)$, assembled from the literature, is indicated by shading in Fig. 2. In the most relevant region below $Q^2 \approx 0.5$ $(\mathrm{GeV}/c)^2$ where quark-core dominance is expected to give way to manifestations of the pion cloud—and where existing data cease—the predictions deviate dramatically. Even the most sophisticated model calculations tend to suffer from strong, hard-to-control cancellations of quark and meson contributions at low virtualities; hence, any additional data point approaching the photon point becomes priceless in pinning down these competing classes of ingredients.

Given that the agreement of our new recoil polarization data with the MAID model is quite satisfactory and that the transverse helicity amplitude $A_{1/2}$ is relatively much better known, we have attempted a model-dependent extraction of the scalar amplitude $S_{1/2}$ at the single value of Q^2 of our experiment. We have performed a Monte Carlo simulation across the experimental acceptance to vary the relative strength of $S_{1/2}$ with respect to the best MAID value for $A_{1/2}$ and made a χ^2-like analysis with respect to our experimentally extracted event sample in P'_x, P_y, and P'_z. Since P'_z was the least reliable of the three due to the systematic uncertainty of its extraction, the analysis relied on the other two components, P'_x and P_y, of which the former turned out to be relatively insensitive to the variation of $S_{1/2}$, leaving us with P_y only. Fixing $A_{1/2}$ to its MAID value and taking $S_{1/2}^{\mathrm{MAID}}$ as the nominal best model value, we have been able to express $S_{1/2}$ from our fit as the fraction of $S_{1/2}^{\mathrm{MAID}}$, yielding

$$S_{1/2} = (0.80^{+0.15}_{-0.20}) S_{1/2}^{\mathrm{MAID}} = (14.1^{+2.6}_{-3.5}) \times 10^{-3}\ \mathrm{GeV}^{-1/2}.$$

This result is shown in Fig. 2.

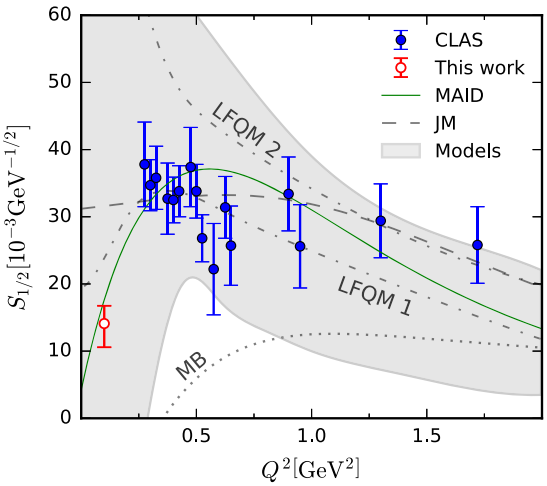

FIG. 2. The scalar helicity amplitude for Roper electroexcitation extracted at $Q^2 = 0.1$ $(\mathrm{GeV}/c)^2$ compared to CLAS measurements [11], MAID [1,16] (solid line), the JLab-MSU parameterization based on the data from Ref. [9] (JM, dashed line), and the light-front quark model results of Refs. [31,39] (LFQM1 and LFQM2, dashed and dash-dotted lines, respectively). The isolated meson-baryon dressing contribution calculated in Ref. [9] is shown by the dotted line (MB). The immense range of other predictions is indicated by shading.

In summary, proton recoil polarization components in the $p(\vec{e}, e'\vec{p})\pi^0$ process in the energy range of the Roper resonance have been measured precisely for the first time. The unitary isobar approach (MAID) based on dressed resonances is superior to the model involving dynamical dressing (DMT), while the SAID analysis disagrees with the data in the longitudinal component. The scalar helicity amplitude $S_{1/2}$ for Roper electroexcitation has been determined at a Q^2 very close to the real-photon point. The extracted value confirms the nonhybrid nature of the resonance, favoring the interpretations of the Roper as an entity characterized by strong meson-baryon dressing, in particular with no need for nonquark degrees of freedom, and supports the models of the Roper in which the interplay of quark and meson contributions results in a small value of $S_{1/2}$. This is a relevant finding by itself, as it validates an important model-independent long-wavelength constraint [40–42] that all scalar helicity amplitudes should go through zero at the pseudothreshold [$Q^2 \approx -0.25$ $(\mathrm{GeV}/c)^2$] where the three-momentum transfer vanishes.

This work was supported in part by Deutsche Forschungsgemeinschaft (SFB 1044). We express our gratitude to the MAMI operators for a dedicated supply of high-quality beam. The authors acknowledge the financial support from the Slovenian Research Agency (research core funding No. P1-0102) and thank Ron Workman and Igor Strakovsky for useful discussions regarding the SAID analysis.

*Corresponding author.
simon.sirca@fmf.uni-lj.si
†Present address: MIT-LNS, Cambridge, MA 02139, USA.

[1] L. Tiator, D. Drechsel, S. S. Kamalov, and M. Vanderhaeghen, Eur. Phys. J. Spec. Top. **198**, 141 (2011).
[2] I. G. Aznauryan and V. D. Burkert, Prog. Part. Nucl. Phys. **67**, 1 (2012).
[3] L. D. Roper, Phys. Rev. Lett. **12**, 340 (1964).
[4] V. Shklyar, H. Lenske, and U. Mosel, Phys. Rev. C **87**, 015201 (2013).
[5] A. V. Anisovich, R. Beck, E. Klempt, V. A. Nikonov, A. V. Sarantsev, and U. Thoma, Eur. Phys. J. A **48**, 15 (2012).
[6] R. A. Arndt, W. J. Briscoe, I. I. Strakovsky, and R. L. Workman, Phys. Rev. C **74**, 045205 (2006).
[7] D. Leinweber *et al.*, J. Phys. Soc. Jpn. Conf. Proc. **10**, 010011 (2016).
[8] C. B. Lang, L. Leskovec, M. Padmanath, and S. Prelovsek, Phys. Rev. D **95**, 014510 (2017).
[9] V. I. Mokeev, V. D. Burkert, D. S. Carman, L. Elouadrhiri, G. V. Fedotov, E. N. Golovatch, R. W. Gothe, K. Hicks, B. S. Ishkhanov, E. L. Isupov, and I. Skorodumina, Phys. Rev. C **93**, 025206 (2016).
[10] V. I. Mokeev *et al.*, Phys. Rev. C **86**, 035203 (2012).
[11] I. G. Aznauryan *et al.*, Phys. Rev. C **80**, 055203 (2009).
[12] A. S. Biselli *et al.*, Phys. Rev. C **78**, 045204 (2008).
[13] I. G. Aznauryan, V. D. Burkert, H. Egiyan, K. Joo, R. Minehart, and L. C. Smith, Phys. Rev. C **71**, 015201 (2005).
[14] I. G. Aznauryan, V. D. Burkert, G. V. Fedotov, B. S. Ishkhanov, and V. I. Mokeev, Phys. Rev. C **72**, 045201 (2005).
[15] A. S. Raskin and T. W. Donnelly, Ann. Phys. (N.Y.) **191**, 78 (1989).
[16] D. Drechsel, S. S. Kamalov, and L. Tiator, Eur. Phys. J. A **34**, 69 (2007).
[17] G. Y. Chen, S. S. Kamalov, S. N. Yang, D. Drechsel, and L. Tiator, Phys. Rev. C **76**, 035206 (2007).
[18] R. A. Arndt, W. J. Briscoe, M. W. Paris, I. I. Strakovsky, and R. L. Workman, Chin. Phys. C **33**, 1063 (2009).
[19] T. Pospischil *et al.*, Phys. Rev. Lett. **86**, 2959 (2001).
[20] J. J. Kelly *et al.*, Phys. Rev. C **75**, 025201 (2007).
[21] J. J. Kelly *et al.*, Phys. Rev. Lett. **95**, 102001 (2005).
[22] H. Merkel *et al.*, Phys. Rev. Lett. **99**, 132301 (2007).
[23] A. Picklesimer and J. W. VanOrden, Phys. Rev. C **35**, 266 (1987).
[24] K. I. Blomqvist *et al.*, Nucl. Instrum. Methods Phys. Res., Sect. A **403**, 263 (1998).
[25] K.-H. Kaiser *et al.*, Nucl. Instrum. Methods Phys. Res., Sect. A **593**, 159 (2008).
[26] M. Dehn, K. Aulenbacher, R. Heine, H.-J. Kreidel, U. Ludwig-Mertin, and A. Jankowiak, Eur. Phys. J. Spec. Top. **198**, 19 (2011).
[27] T. Pospischil *et al.*, Nucl. Instrum. Methods Phys. Res., Sect. A **483**, 713 (2002).
[28] L. Doria, Ph.D. thesis, Johannes Gutenberg-Universität Mainz, 2008, http://d-nb.info/98728844X.
[29] L. Doria *et al.*, Phys. Rev. C **92**, 054307 (2015).
[30] M. Dugger *et al.*, Phys. Rev. C **79**, 065206 (2009).
[31] S. Capstick and B. D. Keister, Phys. Rev. D **51**, 3598 (1995).
[32] Z. Li, V. Burkert, and Z. Li, Phys. Rev. D **46**, 70 (1992).
[33] F. Cardarelli, E. Pace, G. Salmé, and S. Simula, Phys. Lett. B **397**, 13 (1997).
[34] C. S. An and B. S. Zou, Eur. Phys. J. A **39**, 195 (2009).
[35] B. C. Liu and B. S. Zou, Phys. Rev. Lett. **96**, 042002 (2006).
[36] I. G. Aznauryan *et al.*, Phys. Rev. C **78**, 045209 (2008).
[37] T. Bauer, S. Scherer, and L. Tiator, Phys. Rev. C **90**, 015201 (2014).
[38] B. Golli, S. Širca, and M. Fiolhais, Eur. Phys. J. A **42**, 185 (2009).
[39] I. G. Aznauryan, Phys. Rev. C **76**, 025212 (2007).
[40] G. Ramalho, Phys. Rev. D **94**, 114001 (2016).
[41] G. Ramalho, Phys. Rev. D **93**, 113012 (2016).
[42] G. Ramalho, Phys. Lett. B **759**, 126 (2016).